African Journal of Geographical Sciences
Vol. 5 No. 1, 2024 (ISSN: 2786-9741)

Spatio-Temporal Change in Land Use, Land Cover and Land Surface Emissivity in Benin City, Edo State, Nigeria

Courage Onyeka Anyokwu and Toju Francis Balogun

Department of Geography and Regional Planning, University of Benin, Benin City, Edo State
Corresponding author: Email: courageonyex@yahoo.com
Doi: https://doi.org/10.5281/zenodo.13734010

Abstract
Land use-land cover changes are adjudged as major drivers of climate change. They determine the level of Land Surface Emissivity and the consequent thermal conditions. This study examined the impacts of land use land cover change on land surface emissivity of Benin City between 1991 and 2021. It employed a geospatial technique for the data acquisition and spatial analysis. The result showed a spatio-temporal change in urban land uses which led to a remarkable loss in vegetal cover. The trend of depletion in vegetation and changes in land uses was followed by a rise in urban land surface emissivity. Thus, there was a corollary between change in land use land cover and land surface emissivity. Within the period, water body increased by 0.0088 Km^2, the built-up area increased by 34.4587 Km^2 while cultivated area and vegetation reduced by 2.0413 Km^2 and 29.0069 km^2 respectively. Findings also revealed a steady rise in LSE within the period from a range of 0.975-0.987µm in 1991 to 0.986-0.987µm in 2006 and 0.986-0.988µm in 2021. By implication, there was a progressive increase in the land surface emissivity due to changes in land use land cover within the study period. Hence, urban land use land cover dynamics lends credence to urban land surface emissivity which is a precursor to several ecological problems. It becomes necessary to adopt relevant mitigations like afforestation, use of low thermal emissive materials and effective urban planning to curb the emissions.

INTRODUCTION
Global urban revolution has greatly modified natural landscape through the persistent destruction of land cover and the injection of greenhouse gases. It has transformed the natural and serene rural environment into a more anthropogenic one, resulting to changes in the climate characteristics and other environmental problems (Chukwuka and Makinde, 2018). Urban growth is a continuous process of increase in the population, spatial dimension, functions and improvement in infrastructure (Abotutu, 2016). It is usually accompanied by replacement of beneficial natural vegetation with artificial concrete surfaces, reduction of agricultural lands and depletion of natural resources, resulting to increase in emissivity and urban warming (Maryam, 2017).

Urban warming is linked to the heat emanating from the different spatial objects on the earth surface which serve as an important parameter in computing land surface emissivity. All objects at temperature above absolute zero emit thermal radiation. However, for any particular wavelength and temperature, the amount of thermal radiation emitted depends on the emissivity of the object's surface. Therefore, land surface emissivity is the radiant absorption power of a surface or body in the long wave radiation spectrum of a place from the thermal infrared band (Amer, Parham and Bernaz, 2017). It is the measure of the ability of a body to emanate thermal radiation with respect to that emanating from a *black body* of similar temperature (Surjikov, 2010). Thus, it determines the amount of heat that is released into the environment at a given period.

The knowledge of emissivity is important both for accurate non-contact temperature measurement and for heat transfer calculation (Bolstad, 2002). Object with high emissivity has high absorption and objects with lower emissivity emit less light and reflects more light e.g. smooth surfaces. The level of emissivity of any place is determined by its *spatial morphology* (i.e. structure, coverage and metabolism) and *surface fabrics* (i.e. materials and colours) which together dictate the reflectance or emission of radiant heat energy of the sun into the city. Thus, contributing to the building up and intensifying of urban heat by refracting incident light or solar energy through reflection,

making the city relatively warm (Manat, Kazunori and Vivarad, 2012).

Benin City as an urbanizing area has been experiencing urban warming in recent times (Efe, and Eyefia, 2014). The increasing temperature of the city has brought about changes in weather patterns and other heat-related problems. Some scientific research carried out in this regard on Benin City include those of Efe and Eyefia (2014), Okhakhu (2016), Floyd, Oikpor and Ekene (2016), Ukhurebor, Batubo, Abiodun and Enoyoze (2017) and Obiaderi and Thelma (2019) to mention but a few. However, the dynamic nature of the urban climate particularly in the aspect of its thermal conditions has not been fully assessed from all scientific perspectives. More so, these studies did not emphasize the role of land surface emissivity and land use/land cover on the thermal condition of the city. This gap in knowledge demands scientific research that will complement the aforementioned to bridge the development vacuum by addressing the issues identified and recommending relevant strategies for effective urban planning and policy implementation. This will make our cities not only conducive and viable but sustainable.

2.0: MATERIALS AND METHOD

2.1: Study Area

Benin City is the administrative headquarters of Edo State in southern Nigeria. It is located between latitudes 6º 12'N and 6º 28'N and between Longitudes 5º 34'E and 5º 44'E. Its spatial extent is approximately 1,204km^2 cutting across five Local Government Areas including Egor, Ikpoba-okha, Oredo, parts of Uhunmwonde and Ovia North-East. The city has witnessed rapid areal expansion in recent times. In 2008, it was estimated to be 119,539.27ha and was estimated at 1, 3483, 312.14 ha in the year 2020 (Efe and Eyefia, 2014). This shows an urban expansion of 3000hectares every nine years. This area expansion is closely linked to population increase of the city. The population of the city is estimated to be 1,727,000people as of 2020 (Obiaderi and Thelma, 2019), with a growth rate of 3.99% per annum and a population density of 1200/km^2 (World Bank Group, 2021).

Benin City is situated within the tropical equatorial rainy climate, which is characterized by two distinct climatic seasons: the rainy and the dry seasons. The rainy season occurs between April and October occasioned by a few weeks break in August, with an average annual precipitation of about 2025mm (Eruotor, 2014). The mean annual temperature of the city is between 26.1ºc in the rainy season and 28ºc in the dry season (Okhakhu, 2016). The city is drained by three main rivers: Ikpoba river (drains from the north to the south of the City) with a distance flow of 48km, width of 5-11m, depth of 3-8m and a sub-drainage catchment basin of about 722 km^2. On the other side, the Ogba River drains the southwestern part of the City and flows for about 12km with a width of 1-3m, a depth of 1-2m and a catchment area of 40 km^2. In the northwestern portion, River Owigie-Ogbovben, catchment area of 10 km^2, drains from the north east to the south west of the City (Ikhile, 2016).

Benin City is situated in the tropical rainforest belt, which is characterized by giant trees (Eruotor, 2014). The prevailing tropical rainy climate condition has favoured luxuriant plant growth in the area, making its vegetation more of an evergreen forest (Emielu, 2014). The Common tree species found around the area are the Milicia excelsa, Chlorophora excels and Swietenia Macrophylla (Iroko, Obeche and Mahogany). However, in recent times this natural vegetation has been altered by human activities such as lumbering, farming and road construction among others, has led to a secondary re-growth (Ikhuoria, 2016).

The unique position of Benin City in different parts of the country as well as being the state capital, coupled with its commercial potential has attracted financial institutions and industries to the area (Odjugo, Enaruvbe and Isibor, 2015). The economy of the city is more of the public service in the formal sector and commerce in the informal sector. A greater part of the workforce are employed in clerical jobs with a good percentage in the formal employment (Ikhuoria, 1987). Also, trade flourish in the area as many are engaged in the sales of items ranging from household equipment such as electrical and electronics appliances, building materials, and textiles to food items in both open markets and retail outlets across the city. Urban dwellers also engage in crafts such as carpentry, tailoring, brass casting, black smiting and automobile and electrical repairs among others, not neglecting commercial transporters which is also a very common occupation in the area. However, the industrial sector is dominated by the hospitality, entertainment, mining industries and food processing industries and pharmaceutical industries. Small scale farming is also very common around the

metropolitan areas (Odjugo, Enaruvbe and Isibor, 2015).

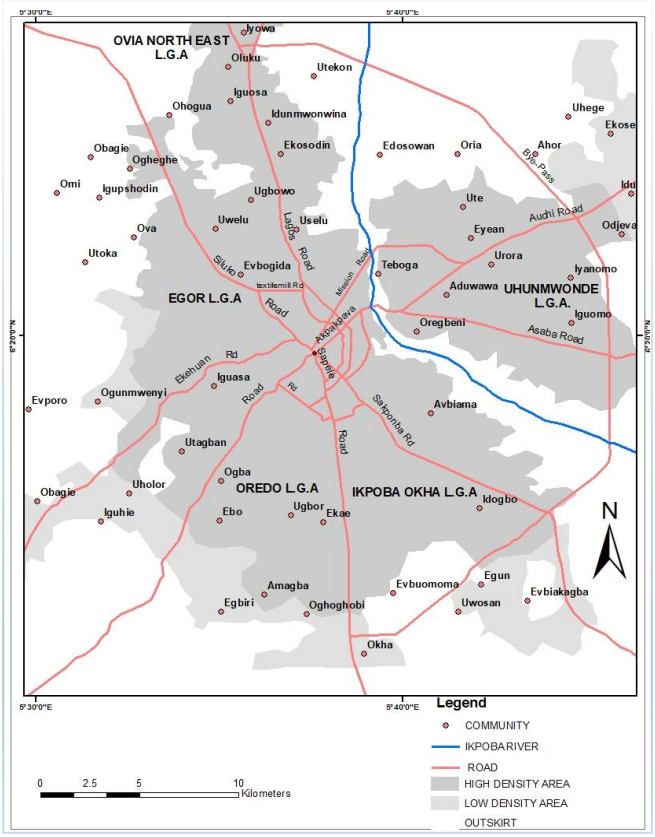

Figure 1: Map of the Study Area
Source: Ministry of Lands and Surveys (2021).

Materials/Methods

This work examines the transition of land use land cover patterns and its effect on land surface emissivity of Benin City. It employed a number of procedures in carrying out the work and this is discussed below.

Data

Remote sensing data were obtained, processed analyzed and Land use/Land cover (LULC) spatial dimension values and Land Surface Emissivity (LSE) values were extracted using geospatial techniques. The data employed are mainly Landsat images and administrative map of the study area. The satellite images were downloaded from the website of the US Geological Survey at www.glcffapp.glcf.umd.edu and NASA website of surface meteorology and solar energy choice at http://www.energycodes.gov. The images were extracted from one scene (path/ row 189/ 056) of Landsat 5TM 1991; Landsat 7 TM 2006 and Landsat 8 ETM+ 2021. The images were all acquired on 24th December. The 30-year period is to allow for noticeable changes in LULC patterns and to effectively evaluate changes in the LSE within the period. Table 1 itemized the characteristics of the image used for the work:

Table 1: Characteristics of Landsat Sensor

Satellite Sensor	Acquisition Date	Spatial Resolution	Format	Band Required
Landsat5 TM	December, 1991	30m	Tiff	3, 4, and 6
Landsat7 ETM	December, 2006	30m	Tiff	4,5,10 and 11
Landsat8 ETM +	December, 2021	30m	Tiff	5,7, 10 and 11

Source: Landsat metadata file

The conversion of the raw data into a usable format to have a valid result involves a series of steps. The ENVI software was employed in the classification process using the supervised classification technique which requires a reconnaissance knowledge of the researcher to train the sample set. The algorithm classifier was used to run all the pixels of the image based on the already defined training set into class. Four basic land use land cover types were identified. They include the built-up, water bodies, cultivation and vegetation. To avoid calculating surface emissivity and vegetation indices of the part of the image outside the study area clipping was carried out to extract the defined area of the satellite image (Bolstad, 2002). Thus, the spatial extent of Benin City was extracted from the image using the shape file from the output of a supervised classification method.

The Landsat image used has Digital Number (DNs) values which are not calibrated and has atmospheric effects and cannot be used for quantitative analysis. Hence image calibration was first carried out. According to Annamaria, Jose, Drazen and Eric (2017), image calibration is basically to correct atmospheric effects and quantize the image into some measure of physical unit. This process of converting the digital number (DNs) of the image was done manually using the ArcGIS Raster Calculator. Landsat 8 thermal constants, and rescaling factor values that are used for LSE are shown in Table 2. These computational values are available in the metadata file. The computation was based on the following procedures:

Conversion to Radiance

$$L_A=M_LQ_{cal} + A_L$$

L_A= TOP Spectral radiance (watts/ (m^2* srad* µm)
M_L= band spectral multiplicative recalling factor from metadata (file value of Radiance band x.
x = the band number
A_L=band specific additive rescaling factor (radiance add band x)
x= band number.
Q_{cal} = quantized and calibrated standard product pixel values (DN: digital number for wavelength).

Variables values were obtained from the metadata file and x is the wavelength band being corrected.

Table 2: Metadata values used for computation

Band Characteristics	Band 10	Band 11
Radiance multi band x.(M_L)	3.3420E-04	3.3420E-04
radiance add band x (A_L)	0.10000	0.10000
$Q_{cal\ (DN)}$	Band10	Band11
K1	774.89	480.89
K2	1321.08	1201.1442

Table 3: Characteristics of the selected image bands

Bands: Landsat5 TM/ Landsat7 ETM	Wavelength range	Spectral Response	Spatial Resolution
1	0.45 - 0.520	Blue – Green	30
2	0.52 – 0.600	Green	30
3	0.63 – 0.690	Red	30
4	0.760 – 0.900	Near – IR	30
5	1.550 – 1.750	Mid – IR	30
6	10.40 – 12.50	Thermal	120
7	2.080 – 2.350	Mid – IR	30
Landsat8 ETM+			
4	0.636 – 0.673	Red	30
5	0.851 – 0.879	Near-infrared	30
10	10.60 – 11.19	Thermal Infrared (TIRS 1)	30
11	10.50 – 12.51	Thermal Infrared (TIRS 2)	30

Sources of Tables 2 and 3: Landsat metadata file
The image to radiance was further converted to the satellite brightness temperature.

Brightness Temperature

Brightness temperature (T) = $\frac{K_2}{\ln(\frac{K_1}{L\Lambda} + 1)}$ - 273.15

Where,

T= at satellite brightness temperature (K)

$L\Lambda$= TOA spectral radiance (watt / (m^2*Srad*μm))

K_1= Specific thermal conversion constant from the metadata (K_1_Constantband_X. where X is the band number 10 or 11)

K_2= band specific thermal conversion constant from the result will serve as input

Estimation of Emissivity

Land surface emissivity is defined as the radiant absorption power of a surface in the wave radiation spectrum Surjikov (2010). The Normalized Difference Vegetation Index (NDVI) which gives the proportion of the vegetation is important in the estimation of emissivity. Thus, the NDVI index value is sensitive to the presence of vegetation on the earth's surface and is also highly correlated with climatic variables, such as precipitation, sunshine, temperature and cloud cover (Mushkin, Balick, and Gillespie, 2005). This value ranges between -1 to +1 and the computation of this index valu use of two bands which are the red band 4 and the infra-red band 5 of the Landsat image (Watson 1992).

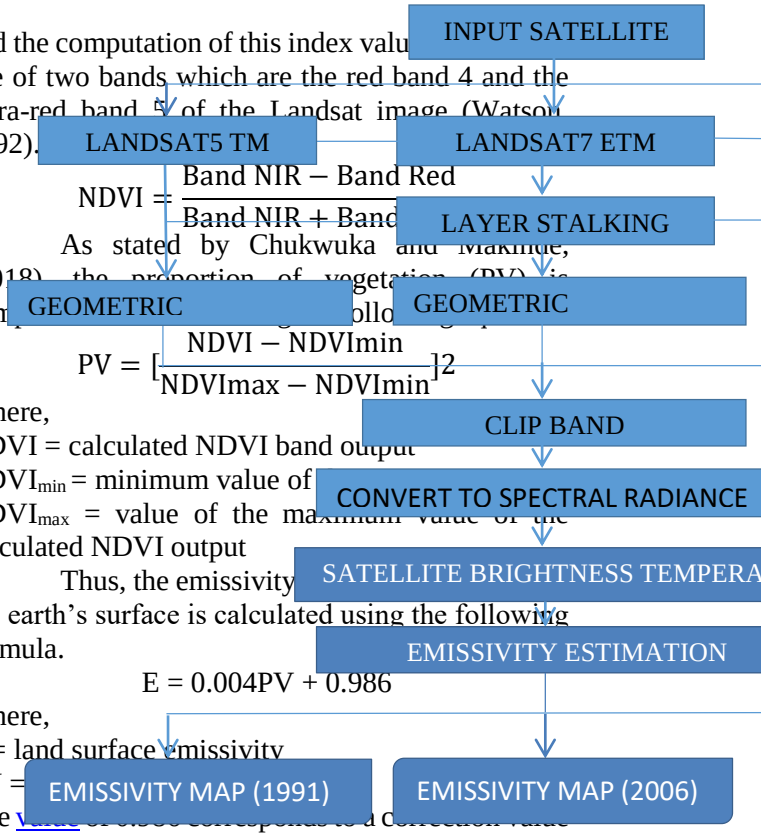

$$NDVI = \frac{Band\ NIR - Band\ Red}{Band\ NIR + Band}$$

As stated by Chukwuka and Makinde, (2018) the proportion of vegetation (PV) is com ollo

$$PV = \left[\frac{NDVI - NDVImin}{NDVImax - NDVImin}\right]2$$

Where,

NDVI = calculated NDVI band output

$NDVI_{min}$ = minimum value of

$NDVI_{max}$ = value of the maximum value of the calculated NDVI output

Thus, the emissivity the earth's surface is calculated using the following formula.

$$E = 0.004PV + 0.986$$

Where,

E = land surface emissivity

PV =

The value of close corresponds to a correction value of the equation.

Figure 2: Schematic representation of data analysis

Statistical Analysis

In order to validate the result of analyzed data, the land surface emissivity values for the three time periods (1991, 2006 and 2021) were extracted from the calibrated Landsat image using ArcGIS application. One-way Analysis of Variance (ANOVA) which is an extension of t-test was used. This becomes necessary when the independent variable also known as factor (expansion of the built up area) consist of more than two groups or conditions within the factor. Thus, the dependent variable is of a ratio measurement scale.

The independent variable is composed of three groups which defined the periods of investigation (1991, 2006 and 2021) with their respective extracted land surface emissivity values. The rationale for using the respective land surface emissivity values is to ascertain if expansion of the built up area corresponds with increase in land surface emissivity. The dependent variable is the land surface emissivity. Since this analysis is based on a single criterion (LSE), the totals, means and sum of squares were computed for each sampled period. Therefore, the independent variable (x) becomes the periods of urban land uses. Numbers as follows:

x_1= built up area in 1991
x_2= built up area in 2006
x_3= built up area in 2021

Thus, the total, mean and sum of squares of land surface emissivity generated from the period of expansion in the built up area are given as:

$\Sigma x1, \Sigma x2, \Sigma x3$ …..…..Σxn ……(3.1)
$\Sigma \bar{x}\ 1, \Sigma \bar{x}\ 2, \Sigma \bar{x}\ 3$ …..…..$\Sigma \bar{x}n$ ……(3.2)
$\Sigma x_1^2, \Sigma x_2^2, \Sigma x_3^2$…….$\Sigma x_n^2$ ……....(3.3)

In One-way ANOVA, we determine differences between means (land surface emissivity generated from the various years) by calculating their variability. The three types of variability are estimated:

i. The variation within each group. ii. The variation between groups.

ii. The total variation of the groups, regardless of the class group to which they belong.

These parameters are determined as follows:

First, the 'grand mean' of the land surface emissivity generated from the periods of expansion of the built up area ($\bar{\bar{x}}$) is computed. The grand mean is given by:

$$x = \frac{\Sigma\Sigma xij}{\Sigma nj}$$

Where: $\Sigma\Sigma x_{ij}$ is the overall total values of independent variable (the three levels of expansion of the built up area) and Σ_{nj} is the overall total case, N.

Secondly, we compute the sums of the sum of squares for each variable. The sums of the sum of squares of land surface emissivity generated from the various years of expansion in built up area. This is given as:

$$\Sigma\Sigma i^2j^2$$

Where: $\Sigma\Sigma i^2j^2$ is the sum of the total of the sum of squares of land surface emissivity generated from the three periods of expansion of the built up of the area.

Thus, the total sum of squares of land surface emissivity generated from the three periods of expansion of the built up area is given as:

$$TSS = \Sigma\Sigma i^2j^2 - N\bar{\bar{x}}^2$$

Where $\Sigma\Sigma i^2j^2$ is the sums of the sum of squares of land surface emissivity generated from the periods of expansion of the built up of the area, N is the overall total case and $\bar{\bar{x}}^2$ is the grand mean of land surface emissivity generated from the periods of expansion of the built up area.

Then the between-group sum of squares, BSS is given as:

$$BSS = [\Sigma_{nj}\ \bar{x}^2] - N\ \bar{\bar{x}}^2$$

Where Σ_{nj} is the number of observations of each group of urbanization, $\bar{x}^2$ is the square of the mean of each group of periods of expansion of the built up area, N is the overall total case of expansion of the built up area periods and $\bar{\bar{x}}^2$ is the square of the grand mean.

The within-group sum of squares (WSS) is expressed as:

$$WSS = TSS - BSS$$

Consequently, the mean square average that is known as variance estimates is computed. The between-group variance estimate is given by:

$$S_B^2 = \frac{BSS}{K-1}$$

On the other hand, the within-group variance estimate is given by:

$$S_W^2 = \frac{WSS}{N-K}$$

Where N is the overall total case of periods of expansion of the built up area and K is the number of groups of expansion of the built up area periods, which is in this case 3.

The ratio between the variance estimates is known as the Snedecor's variance ratio test or Snedecor's *F*, where:

$$F = \frac{SB2}{SW2}$$

The Snedecor's *F* tests the equality of the mean of the land surface temperature. The confidence level of 0.05 was adopted.

Classification Accuracy Assessment

The accuracy assessment for the classified images becomes imperative as it helps to determine the level of accuracy of analyzed data in relation to the referenced data. The reference data used for the accuracy assessment was based on ground trothing which was also validated with high resolution satellite images. A total of 100 randomly distributed ground truth points within the limit of city were selected. The points generated were based on stratified random sampling type and stratification was proportionate across all classes. These points were used to compute the confusion or error matrix (EM) for the classified Landsat imagery, based on Kappa coefficient with which the outcomes of each classification for each year were compared. This was done by using the validation classified areas.

Confusion matrix is used to compare the classified pixels in the classified image to a reference authentication dataset in the case of a high-resolution image (Meng, Xin and Chen, 2016). Confusion matrix tables required for the assessment were generated with pixel counts organized in categories of rightly classed and incorrectly classed; the classification does address the number or amount of rightly classed pixels as well as those that are wrongly classified and their specific classes (Bolstad, 2002). As such, it became possible to appreciate the probability of any systematic error in the classification. The overall accuracy is at a maximum of 100 percent, however accuracy of 80% and above can be considered to be good outputs (Pavel, 2005). Assessing both the producer and user accuracy was made possible by the confusion matrix. This is made possible by a division of the rightly classed pixels with that of the total classed pixels for every category. The percentage of over and under classification is also determined here.

Therefore, the total of rightly classified pixels becomes the overall accuracy (Watson, 1992). Information obtained from accuracy assessment helps in unveiling the extent to which the dataset relates to the validation data. The kappa coefficient can be calculated for further analysis of such agreement. The kappa Coefficient is centered on chance agreement between the datasets and the overall accuracy. It facilitates an improved appreciation of the classification scheme and helps to reveal whether the results were achieved better than it would have been if it goes strictly by chance. This is important because it helps to understand whether the agreement that exist between the classification dataset and the validation dataset are due to chance alone (Bolstad, 2002). Kappa is computed using the mathematical expression presented in equation:

$$K = \frac{\text{Observed} - \text{Expected}}{1 - \text{Expected}}$$

However, where observed is equal to overall accuracy and the expected is calculated from the total for rows and total for columns. The overall accuracy based on chance was calculated using the mathematical expression presented in equation:

$$CA = \frac{\text{Product Matrix}}{\text{Cummulative Sum of Product Matrix}}$$

RESULTS AND DISCUSSION

The results of the image analysis are presented in tables and maps. First, the Land Use Land Cover spatio-temporal change of Benin City for the period under study was discussed. Thereafter, the Land Surface Emissivity was attended to.

Land Use and Land Cover of Benin City between 1991, 2006 and 2021

Land use and land cover analysis provide a comprehensive engagement of the use of land in a given geographical location (Olayiwola and Igbavboa, 2014) and the intensiveness in the use of land by man is subject to the dynamic process of urbanization. Table 4 shows the land use land cover patterns of Benin City within a span of 30years (1991, 2006 and 2021).

The value of the built up area in 1991 was computed to be 116.67km^2. On the other hand, the cultivated area accounted for 54.60km^2, vegetation was computed to be 1105.85km^2 and water body was 0.1521km^2. This indicates that vegetation occupied a larger part of the area (86%) followed by

the built-up area (9.14%), then the cultivated area (4.27%), while the water body has the least portion of the total area (0.01%). This is cartographically presented in Figure 3.

The computed value in 2006 shows that the built-up area was 203.67km^2, the cultivated area was 190.95km^2; the vegetated area was calculated to be 930.02km^2 while the water body was 0.40km^2. Just like 1991, vegetation occupied the greater part of the study area (70.19%) followed by the built-up area which occupied 15.37% of the total area. Also, the cultivated area was estimated to 14.41%, while the least portion of the land was occupied by water body (0.03%). This is shown in Figure 4.

The computed land use and land cover area dimension in 2021 shows that the built-up area occupied 633.55km^2, cultivated area occupied 23.98km^2, vegetation was estimated to be 670.75km^2 while water body occupied 0.28km^2. It is quite obvious that vegetation account for highest land cover of about 50.49% , followed by built up area which account for 47.69% , cultivation with a percentage of 1.80% while water body account for the least with a percentage of 0.02. This is displayed in Figure 5.

Table 4: Land Use and Land Cover (Km^2) of Benin City between 1991, 2006 and 2021

LU/LC Types	Year A (1991)	Year B (2006)	Year C (2021)	Magnitude of Change (1991-2006)	Magnitude of Change (2006-2021)	Magnitude of Change (1991-2021)
Built-up Area	116.6661	203.67	633.546	87.0039	429.876	516.8799
Vegetation	1105.852	930.0195	670.7484	-175.8323	-259.2711	-435.1034
Cultivated Area	54.5958	190.9539	23.976	136.3581	-166.9779	-30.6198
Water Body	0.1521	0.4005	0.2844	0.2484	-0.1161	0.1323

Source: Author, 2022.

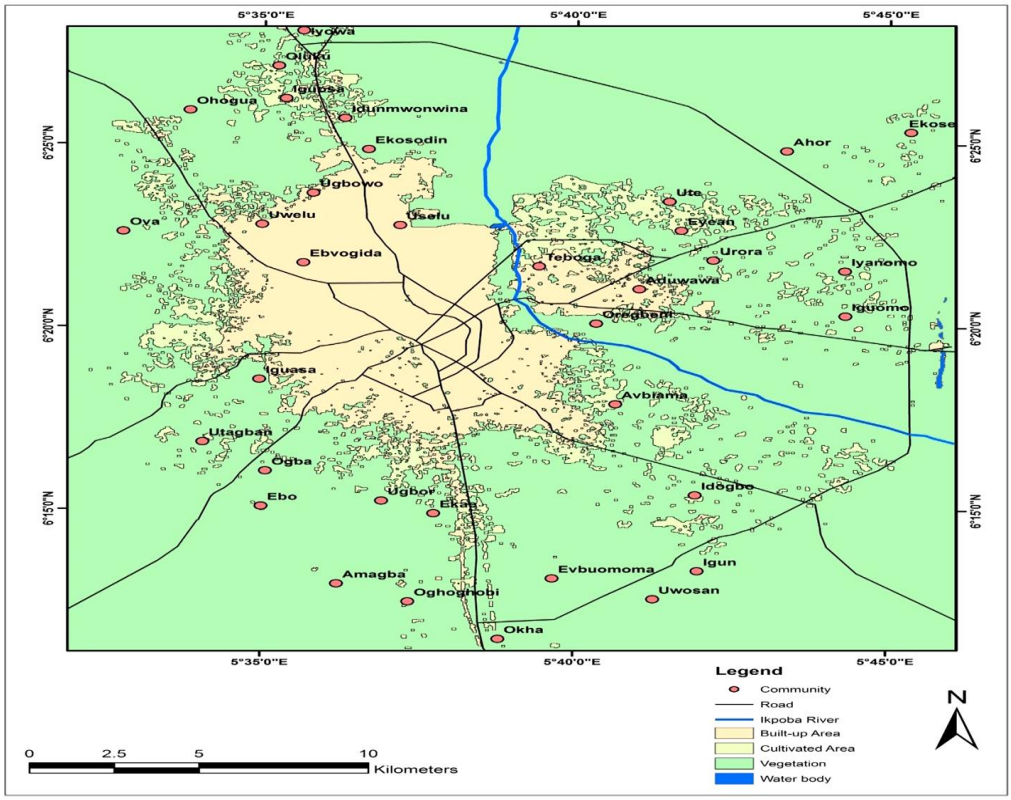

Figure 3: Land Use/Land Cover Profile of Benin City in 1991
Source: Author, 2022.

Accuracy=86.9396%; Kappa coefficient=0.7704

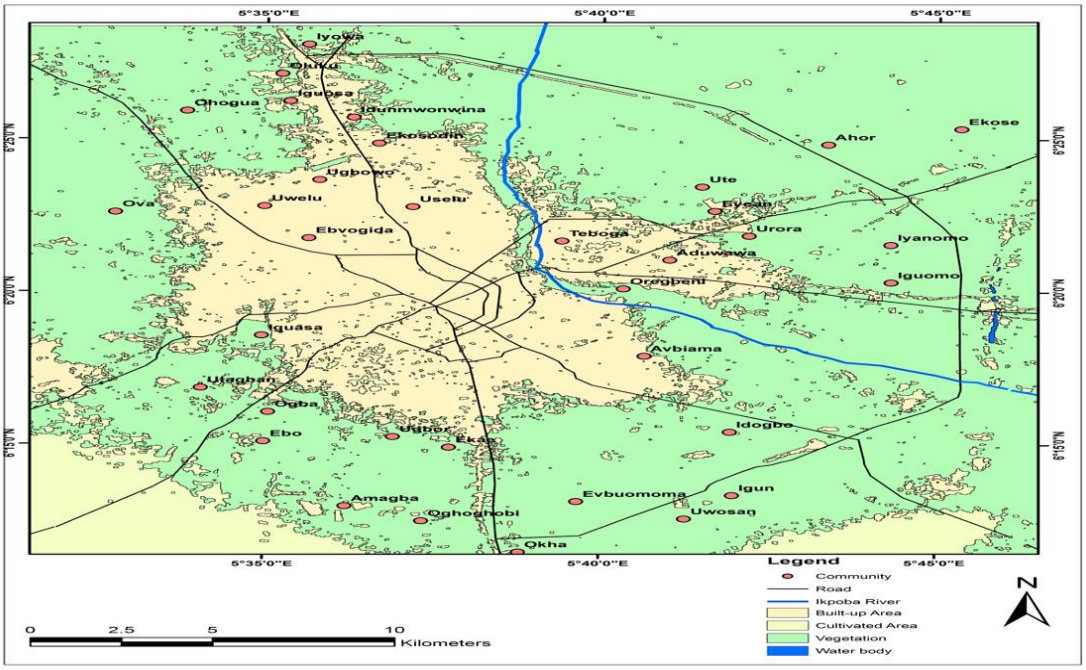

Figure 4: Land Use/Land Cover Profile of Benin City in 2006
Source: Author, 2022.
Accuracy=91.5218%; *Kappa coefficient= 0.8544*

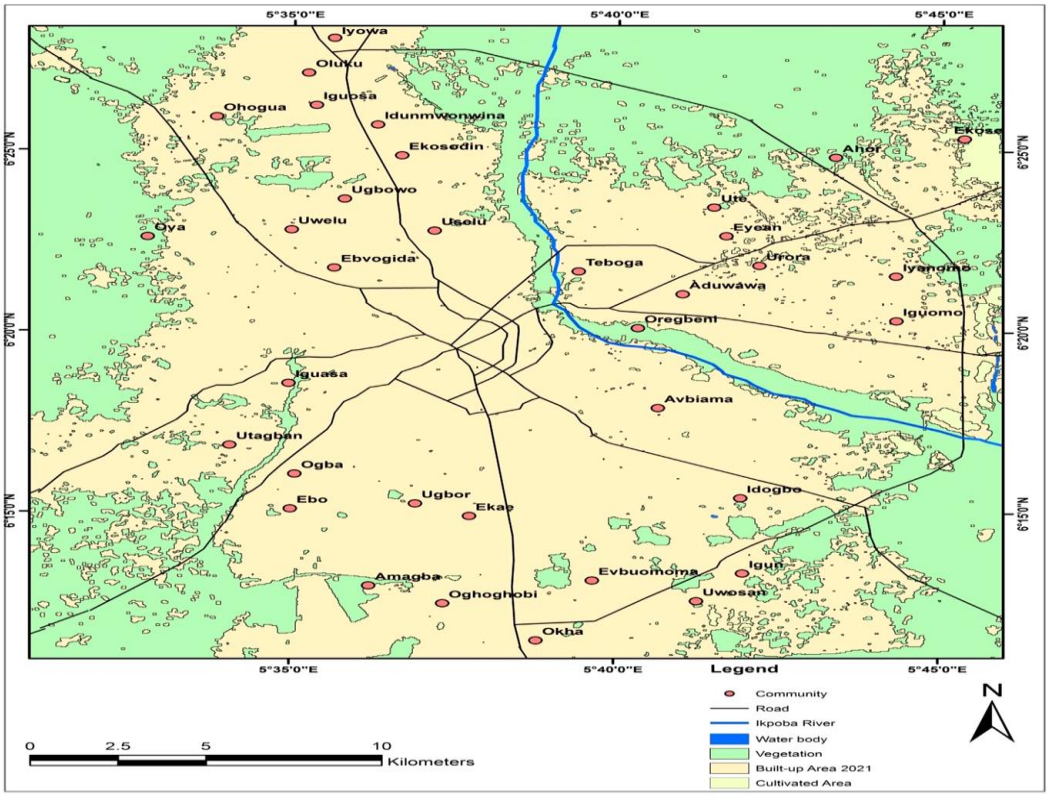

Figure 5: Land Use/Land Cover Profile of Benin City in 2021
Source: Author, 2022
Accuracy=92.3151%; *Kappa coefficient=0.8845*

Change in Land use/Land Cover Pattern of Benin City between 1991 and 2021

The magnitude and rate are paramount when analyzing the spatio-temporal change of any geographical area. Analysis of the magnitude and rate of change was carried out to ascertain the level of change in the spatial dimension of the various land uses and land cover of the area within the period under investigation. The result is displayed in Table 5.

Table 5: Magnitude and Rate of LULC Change (Km^2) in Benin City between 1991 and 2021

LU/LC Type	Magnitude of change (1991-2006)	Magnitude of change (2006-2021)	Magnitude of change (1991-2021)	Rate of change (1991-2006)/N	Rate of change (2006-2021)/N	Rate of change (1991-2021)/N
Built-up Area	87.0039	429.876	516.8799	5.8003	28.6584	34.4587
Vegetation	-175.8323	-259.2711	-435.1034	-11.7222	-17.2847	-29.0069
Cultivated Area	136.3581	-166.9779	-30.6198	9.0905	-11.1319	-2.0413
Water Body	0.2484	-0.1161	0.1323	0.0166	-0.0077	0.0088

Source: Author, 2022.

Magnitude and Rate of Change in Land use/Land cover pattern between 1991 and 2006

The magnitude of land use and land cover change as depicted in Table 5 above shows that the magnitude of change that occurred between 1991 and 2006 for the built-up area was 87.0039 km^2. This implies that the built-up area for 15 years increased by 87.0039km^2. However, the rate of change for this same period was computed to be 5.8 km^2 per annum. For the same period, the magnitude of vegetation change was -175.8323 km^2. Indicating that vegetation has decreased by 175.8323km^2 for the 15 years period. The rate of change was calculated to be -11.7222 km^2 per annum. In other words, vegetation decreased at the rate of 11.7 km^2 annually. Also, the magnitude of change for the cultivated area was computed to be 136.3581 km^2. For the period of 15 years, the cultivated area increased by 136.3581 km^2. While its rate of change was computed to be 9.1km^2 per annum indicating that cultivated area increased by 9.1km^2 annually within the period. Similarly, the magnitude of change for water body was computed to be 0.2484km^2 with a rate of change of 0.016km^2. The annual increase of water body in the area is negligible when compared to the change in magnitude for other land use land cover types in the study area.

Magnitude and Rate of Change in Land use/Land cover pattern between 2006 and 2021

Tables 5 show the magnitude of land use and land cover change between 2006 and 2021. The information depicted in the tables shows that the change in magnitude for the built-up area within the period is 429.8760 km^2, with a rate of change of 28.7 km^2 per annum. The built-up area within a span of 15 years witnessed an increase in spatial dimension of about 429.8760 km^2 (approximately 430 km^2). Similarly, vegetation has a magnitude of change of -259.2711 km^2 and a rate of change of -17.3km^2 per annum. Vegetation experienced a decrease within the period. This clearly shows that within this period some portion of the vegetation gave way to other land uses. The magnitude of change for the cultivated area was computed to be -166.9779 km^2 and the rate of change of -11.1 km^2. Cultivated land decreased and gave way to other land uses. For the water body, the magnitude of change was estimated to be -0.1161 km^2 with a rate of change of -0.01 km^2. Water bodies had a negligible decrease within the period.

Magnitude and Rate of Change in Land use/Land cover pattern between 1991 and 2021

A notable change in land use /land cover was observed in Table 5 between the periods of 1991 to 2021 which is a period of 30 years. As contained in the Table, the change in magnitude for the built-up area was 516.8799 km^2, while the rate of change was computed to be 34.5 km^2 per annum. The observed information portrays an increase in the size of the built-up area within the period of 30 years. Similarly, for the vegetated area, the magnitude of change was observed to be -435.1034km^2 and the rate of change -29km^2 per

annum. It was observed that the vegetation of the area decreased between the aforementioned periods of 30 years. The magnitude of change for the cultivated area was observed to be -30.6198 km^2 with a rate of change of -2.0 km^2. By implication, the cultivated area decreased within the 30 years span. While the observed magnitude for water body was estimated at 0.1323km^2 with a rate of change of 0.01km^2. The change in magnitude and the rate of change for water body tends to be negligible within the period.

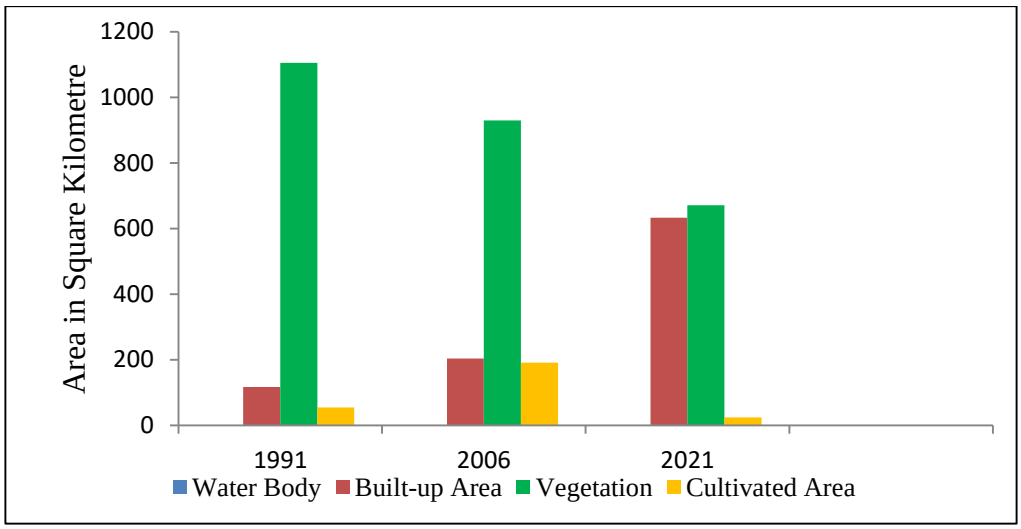

Figure 6: Spatio-Temporal changes in Land use/Land cover of Benin City (1991-2021)
Source: Author, 2022

Land Surface Emissivity of Benin City

Land Surface Emissivity is the heat emanating from the different spatial objects on the earth's surface. To determine the relationship between land use land cover and land surface emissivity in Benin City, land surface emissivity analysis was carried out.

Land Surface Emissivity of Benin City in 1991

The land surface emissivity of the study area in 1991 as displayed in Figure 7 shows that the built up area of the city has a higher emissivity value of approximately 0.987μm, while other land uses such as vegetation, water bodies and cultivated areas have lower emissivity values less than 0.975μm. Higher emissivity values indicate an expansion of the built up area of the city as it encroach into other land uses like vegetation and cultivated areas.

Land Surface Emissivity of Benin City in 2006

An emissivity value of 2006 processed image is shown in Figure 8. The visual representation depicts that the emissivity values within the core centre of Benin City were higher (approximately 0.987μm) when compared to the values of the other parts of the city (less than 0.986μm). This implies decrease in emissivity values as one moves away from the core of the city towards the suburb. Thus, in contrast to the emissivity of Figure 7, it could be seen that the emissivity value of Figure 8 tends to have increased in spatial dimension in relation urban expansion and encroachment of the built up area into other land uses and land cover of the area. In other words, the slight difference in LSE values of the core region and the suburbs is a clear indication that urbanization is fast spreading to all areas.

Land Surface Emissivity of Benin City in 2021

Given the spatial-temporal change in land surface emissivity, which the study seeks to examine for a period of 30years, the LSE of the 2021 image was processed and displayed in Figure 9. The observed information contained in the map shows a high increase in emissivity values over a wider sphere of the built-up area in relation to changes in intensiveness in urban land use and land cover of the study area. The visual representation shows that the emissivity values of the city core centre were higher (approximately 0.988μm) when compared to the values of the other parts of the city (approximately 0.987μm). Similarly, in contrast to the emissivity of 1991 and 2006 the higher emissivity values tend to

cover a wider geographical space due to an increase in urbanization.

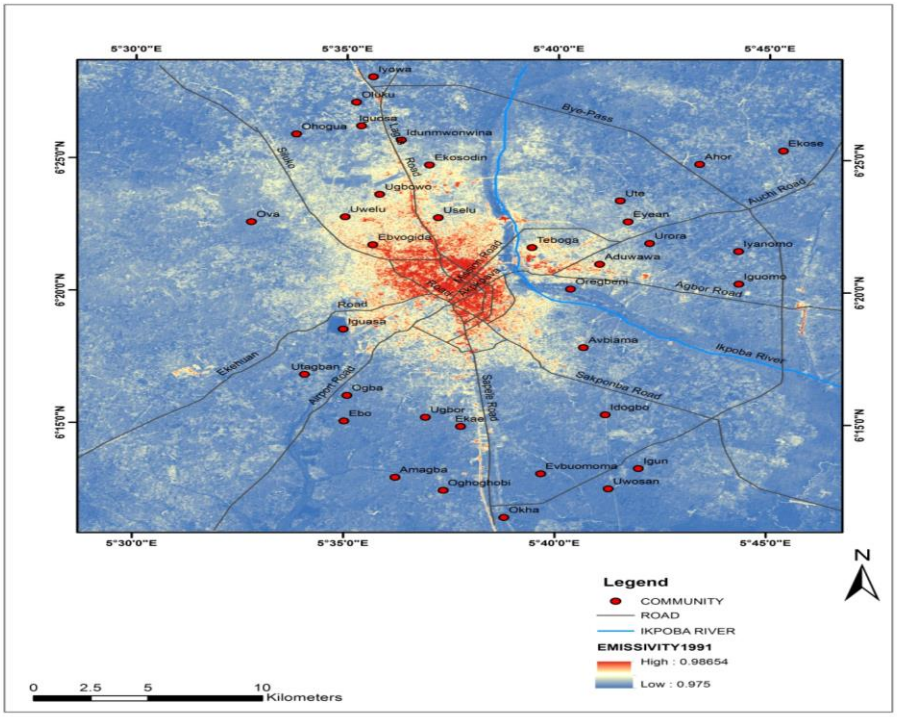

Figure 7: Land Surface Emissivity of Benin City, 1991
Source: Author, 2022

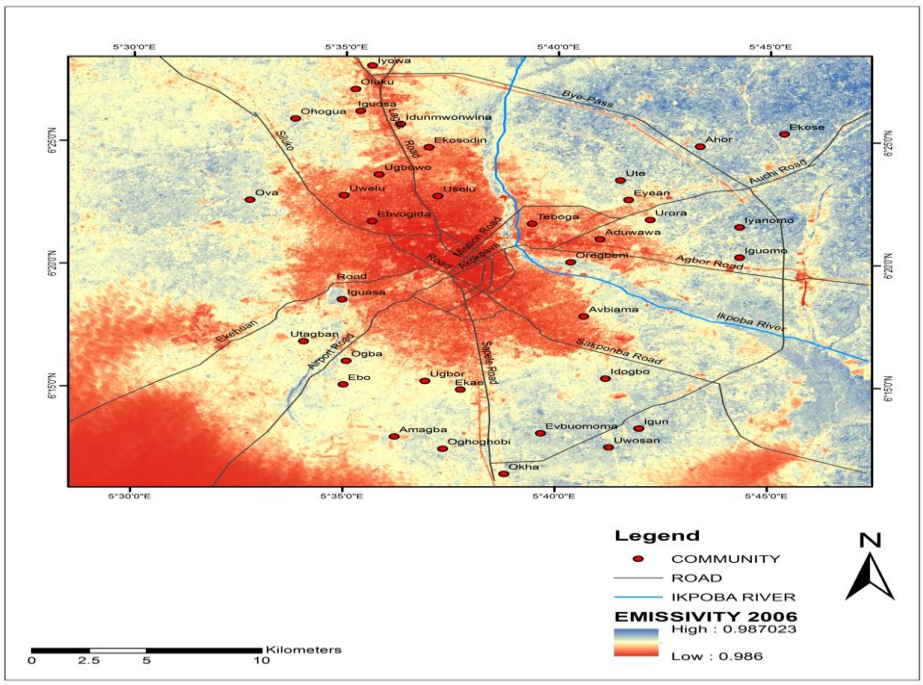

Figure 8: Land Surface Emissivity of Benin City, 2006
Source: Author, 2022

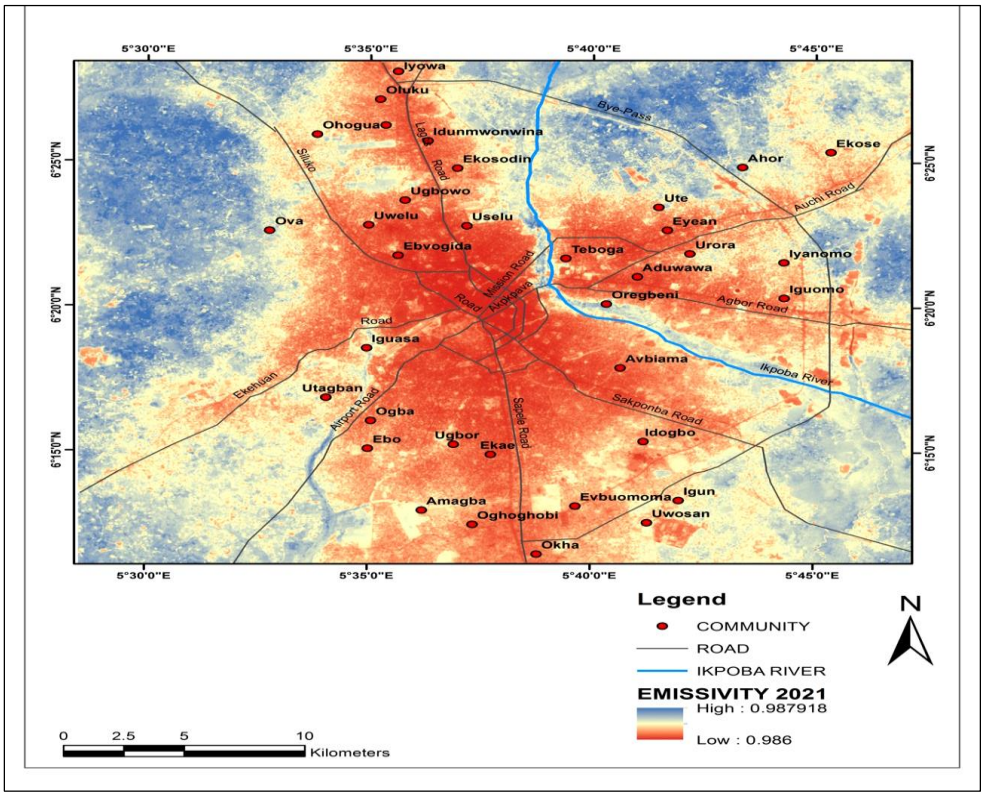

Figure 9: Land Surface Emissivity of Benin City, 2021
Source: Author, 2022

Table 6: Response of Land Surface Emissivity to changes in Land use/Land cover of Benin City

Urban Land uses	1991	2006	2021	Rate of Change (1991-2006)	Rate of Change (2006-2021)	Rate of Change (1991-2021)
Built-up Area	116.6661	203.6700	633.5460	5.8003	28.6584	34.4587
Vegetation	1105.8518	930.0195	670.7484	-11.7222	-17.2847	-29.0069
Cultivated Area	54.5958	190.9539	23.9760	9.0905	-11.1319	-2.0413
Water Body	0.1521	0.4005	0.2844	0.0166	-0.0077	0.0088
Maximum Land Surface Emissivity (μm)	0.98654	0.987023	0.987918	0.000483	0.000895	0.001378

Source: Author, 2022

Table 7 clearly shows the relationship between the various land uses and land surface emissivity of Benin City between 1991 and 2021. The table shows clearly that the built-up area of Benin City increased by 5.8km^2 annually between 1991 and 2006. There was also a noticeable increase in cultivation and water bodies within the period. However, there was a substantial reduction in vegetation of 11 km^2 annually with trade-offs to urban expansion, which increased 0.000483μm in LSE per annum. Similarly, between 2006 and 2021, the depletion in vegetation further increased to about 17 km^2 per annum. This was followed by a decrease in cultivation and water bodies respectively. The depletion in these land use/land cover types could be attributed to the expansion in the built-up area of approximately 29km^2, which led to an increase in its land surface emissivity of about 0.000895μm per annum within the period. Therefore, it could be inferred that within the 30 years period (1991-2021) there was a reduction in vegetation of 29km^2, a reduction in cultivated area

of about 2km^2 and an increase in the built-up area of about 34km^2. The increase in water body is however negligible. These changes in land use /land cover types also resulted in a 0.001378 μm increase in its land surface emissivity in the area. This is an indication of a reduction in absorbency materials such as vegetation which absorb solar radiation and convert it to internal energy through photosynthesis. Conversely, as the built-up area increases there is an increase in objects that attract and retain thermal energy, thus leading to increase in emissivity.

Therefore, to validate the response of land surface emissivity to expansion of the built up area of Benin City between 1991, 2006 and 2021, Analysis of Variance (ANOVA) test was conducted. The input data were generated from Landsat 5TM, 7ETM and 8ETM+ (*see Table 1*). The output result as depicted in Table 8 shows that the mean land surface emissivity for 1991 was 0.91 (S.D=1.4724), the mean LSE for 2006 was 0.987 (S.D=1.6133) and the mean LST for 2021 was 0.994 (S.D=1.5942).

Table 7: ANOVA Descriptive Table on Land Surface Emissivity changes

					95% Confidence Interval for Mean			
	N	Mean	Std. Deviation	Std. Error	Lower Bound	Upper Bound	Minimum	Maximum
Year 1991	1156	.91	1.4724	.0433	.417	.587	.0	.98
Year 2006	4359	.94	1.6133	.0244	.027	.123	.0	.987
Year 2021	5636	.95	1.5942	.0212	.541	.625	.0	.994
Total	11151	2.8	2.4029	.0228	.709	.799	.0	

Source: Author, 2022

A significant difference in mean was observed to be F (11150) =7165.617, P<0.000 (see table 8). Therefore, since the significant level is less than the adopted confidence level of 0.05 it implies that there is a significant difference in the mean land surface emissivity of Benin City for the period under between 1991, 2006 and 2021. This goes to show that as Benin City increased in the built up area within the period and its surface emissivity (LSE) increased respectively. Again, the mean land surface emissivity computed from satellite images of 1991, 2006 and 2021 were computed to be 0.981 μm, 0.986 μm and 0.987 μm respectively.

Table 8: ANOVA Table on Land Surface Emissivity values

	Sum of Squares	Df	Mean Square	F	Sig.
Between Groups	36212.044	2	106.022 2.527	7165.617	.000
Within Groups	28168.674	11148			
Total	64380.718	11150			

Source: Author, 2022

Again, Post-hoc analysis was also carried out to ascertain the difference in mean of land surface emissivity between the designated periods (1991, 2006 and 2021). Table 10 shows the output of the post-hoc (multiple comparisons) analysis of the data. From the result, there was a remarkable difference in the mean of land surface emissivity between 1991 and 2006. Also, a significant difference in land surface emissivity was observed between 2006 and 2021. Similarly, a mean difference in land surface emissivity was also observed between 1991 and 2021. By implication, as the built up area increase spatially over the years, the land surface emissivity increased progressively. It could be inferred that there is a relationship between spatio-temporal change in land use land cover and land surface emissivity.

Table 10. Post-Hoc analysis on response of Land Surface Emissivity to expansion of Built up Area

(I)Lst_year values	(J) Lst_year values	Mean Difference (I-J)	Std. Error	Sig.	95% CI Lower Bound	95% CI Upper Bound
year 1991	year 2006	-5.5734*	.0526	.000	-5.697	-5.450
	year 2021	-6.0812*	.0513	.000	-6.202	-5.961
year 2006	year 1991	5.5734*	.0526	.000	5.450	5.697
	year 2021	-.5078*	.0321	.000	-.583	-.433
year 2021	year 1991	6.0812*	.0513	.000	5.961	6.202
	year 2006	.5078*	.0321	.000	.433	.583

*. The mean difference is significant at the 0.05 level.
Source: Author, 2022

CONCLUSION

The findings of this work showed an increase in the land surface emissivity values over time in response to changes in Land use and Land cover patterns over time. Within the 30years period (1991-2021), there was a rapid expansion of approximately 516.9 Km^2 in the built-up of the city, which led to 435.1Km^2 reduction in urban vegetation and 30.6198 Km^2 reduction in the cultivated areas. Changes in land use/land cover patterns led to a steady rise in land surface emissivity values from 0.98654μm in 1991 to 0.987918μm in 2021, which is approximately 0.001378μm increase. This could be attributed to the reduction in vegetation or land cover type coupled with an increase in built-up areas evident with clusters of tall concrete buildings, tare roads, dense industrial activities, commercial activities and an increase in the flow of traffic, which intensifies the temperature of Benin City as in most cities of the world with high urbanization rates (Caselles., Colleagues, Valor and Rubio, 1995). This helps to further consolidate the fact that changes in Land use and Land cover patterns have impacts on the land surface emissivity of an area as noted in the works of Weng (2001) and Manat, Kazunori and Vivarad, (2012). Therefore, Land use and Land cover changes have a corollary effect on land surface emissivity within the urban sphere of a city, which tends to differ from those observed in the suburb. It is important to know that urbanization will continuously elicit changes in Land use and Land cover patterns, which will in turn manifest in the land surface emissivity within the built-up area, this is because intense socio-economic activities will always continue in other to meet the demand of the ever-increasing urban population. Consequent upon these is the increase in surface temperature which acerbate urban heat inland and the problems it may portend (such as urban warming, increase in cases of heat-related diseases and physiological discomfort to mention but a few). It, therefore, becomes necessary to adopt necessary mitigation, which includes the use of low emissive materials for buildings and afforestation/re-afforestation to complement vegetal loss, efficient land use division in urban planning practice and the introduction of alternative sources of energy to reduce the reliance on fossil fuel and firewood which all contribute to upsurge land surface emissivity.

REFERENCES

Abotutu, A.A. (2016).The impact of urbanization on the vegetation of Abraka and its environs. *African Journal of Environmental Studies, 2,* 16-44.

Adebayo, W.O. (2007). Heat Island and Oasis, effect of vegetative canopies: A micrometeorological investigation. *International Journal of Urban and Region Affairs, 1(1), 35-40.*

Amer, k. Parham, P., & Behnaz, B. (2017). Land use analysis on land surface temperature in urban areas using geographically weighted regression and land sat 8 imagery, case study: Tehran, Iran. *The international archives of the photogrammetry, remote sensing and spatial information sciences, volume XLII-4/WA,*

Annamaria, L., Jose AS., Drazen S. & Eric, A. (2017). The urban heat island effect in the city of Valencia: A case study for hot summer day. *Journal of urban science. 2(1):1-18*

Bolstad, P. (2002). GIS Fundamentals: A first text on Geographic Information Systems. *Eider Press, White Bear Lake, 89-109*

Mushkin, A., Balick, L.K. & Gillespie, A.R (2005). Extending surface temperature and emissivity retrieval to the mid-infrared (3-5 μm) using the multispectral thermal image (MTI). *Journal of remote sensing of the environment,* 9(1), 41-45

Caselles, V., Colleagues, C., Valor, E. & Rubio, E. (1995). Mapping land surface emissivity using AVHRR data: application to La Mancha, Spain. *Remote Sensing Review 12(3-4), 311-333.*

Chukwuka, A. F. & Makinde, E.O. (2018). Land surface temperature mapping using geoinformation Techniques. *Journal of remote sensing of the environment, 32(5), 86-166.*

Efe, S.I. & Eyefia, A.O. (2014). Urban warming in Benin City, Nigeria. *Atmospheric and climate sciences, 4, 241-252.*

Eliasson, I. (1996). Urban nocturnal temperatures, street geometry and land use. *Atmospheric environment 30(3), 379-1379*

Elise, S., Xiaopu, S. & Durwood, Z. (2010). Enhancing urban albedo to fight climate change and save energy. *Journal of Sustainable Development in the Urban Environment,* 11(1), 6-32

Eruotor, S. (2014). *Geography made simple; senior school Geography*. Tonad Publication.

Fabeka, B.B., Balogun, I.A., Adegboyega, S.A. & Faleyimu, O.I. (2018). Spatio-temporal variability in land surface temperature and its relationship with vegetation types over Ibadan, South West Nigeria. *Journal of Atmospheric and Climate Science, 8(3), 316-333*

Ikhile, C.I. (2016). Geomorphology and hydrology of the Benin region, Edo State. *International Journal of Geosciences, 07(02), 144-157.*

Ikhuoria, A.I. (1987). Rapid urban growth and urban land use patterns in Benin City, Nigeria. *Land use policy, 01(4), 62-75.*

Lambin, F.F., & Ehrlich, D. (1996). The surface temperature-vegetation index space for land use and land cover change analysis. *International Journal of Remote Sensing 17(3), 463-487.*

Manat, S. Kazunori, H. & Vivarad, P. (2012). Assessing the impact of urbanization on urban thermal environment: A case study of Bangkok Metropolitan. *International Journal of Applied Science and Technology, 2(7).*

Meng, L., Xin, C. & Chen, X. (2016). Method of land cover classification accuracy assessment considering edges. *Journal of Earth Sciences*, 9(2)23-39

Obiaderi, N.U. & Thelma, E.I. (2019). Analysis of daily average temperature of Benin City using the two parameter Weibull model. *Nigerian Association of Mathematical Physics*, 4(19) 65-71

Odjugo, P., Enaruvbe, G. & Isibor, H. (2015). Geospatial approach to spatio-temopral pattern of urban growth in Benin City, Nigeria. *African Journal of Environmental Science and Technology, 9(3), 166-175.*

Okhakhu, P.A. (2016). Assessment of the urban climate of Benin City, Nigeria. *Journal of Environment and Earth Science, 6(1), 131-143.*

Olayiwola, A. & Igbavboa, O. (2014). Land use dynamics and expansion of the built up area in Benin City, Nigeria. *Mediterranean Journal of Social Science, 5.*

Spence, M., Annez, P.C. & Buckley, R.M. (2009). Urbanization and growth; *World Bank, Washington*. 2(3)22-29

Surjikov, S.T. (2010). Coupled radiation, convention and conduction. *Thermomedia,* 2(2)8-23

Watson, K. (1992). Spectral method for measuring emissivity. *Remote sensing of the environment 42(2), 113-116*

Weng, Q. (2001). A remote sensing-GIS evaluation of urban expansion and its impact on the temperature in the Zhujiang Delta, China. *International Journal of Remote Sensing 22(10), 1999-2014.*

World Bank Group (2021). Climate change action plan: Climate and risk disaster screening. Climate Research Unit. International Bank for Reconstruction and Development. *https//www.worldbank.org/country/Nigeria /benincity*

Zhao-Liang, L., Hua, W. & Ning, W. (2013). Land surface emissivity retrieval from satellite data. *Journal of remote sensing, 2(4),23-45*